Part III:

Chapter 9. Evaluation and respresntation of microtexture data

Introduction

Difference between macrotexture and microtexture measurements lies on the number of measured grains. The number of grains using x-ray is much larger than that using EBSD.

The most valuable aspect of microtexture is the direct link that provides orientation and microstructure. Orientation data are accompanied by a record of sampling coordinates in the microstructure, and the location of these individual data points.

Preferred orientation (Texture) analysis: Grains

Orientation presentation (OP): Microstructure and pole figure

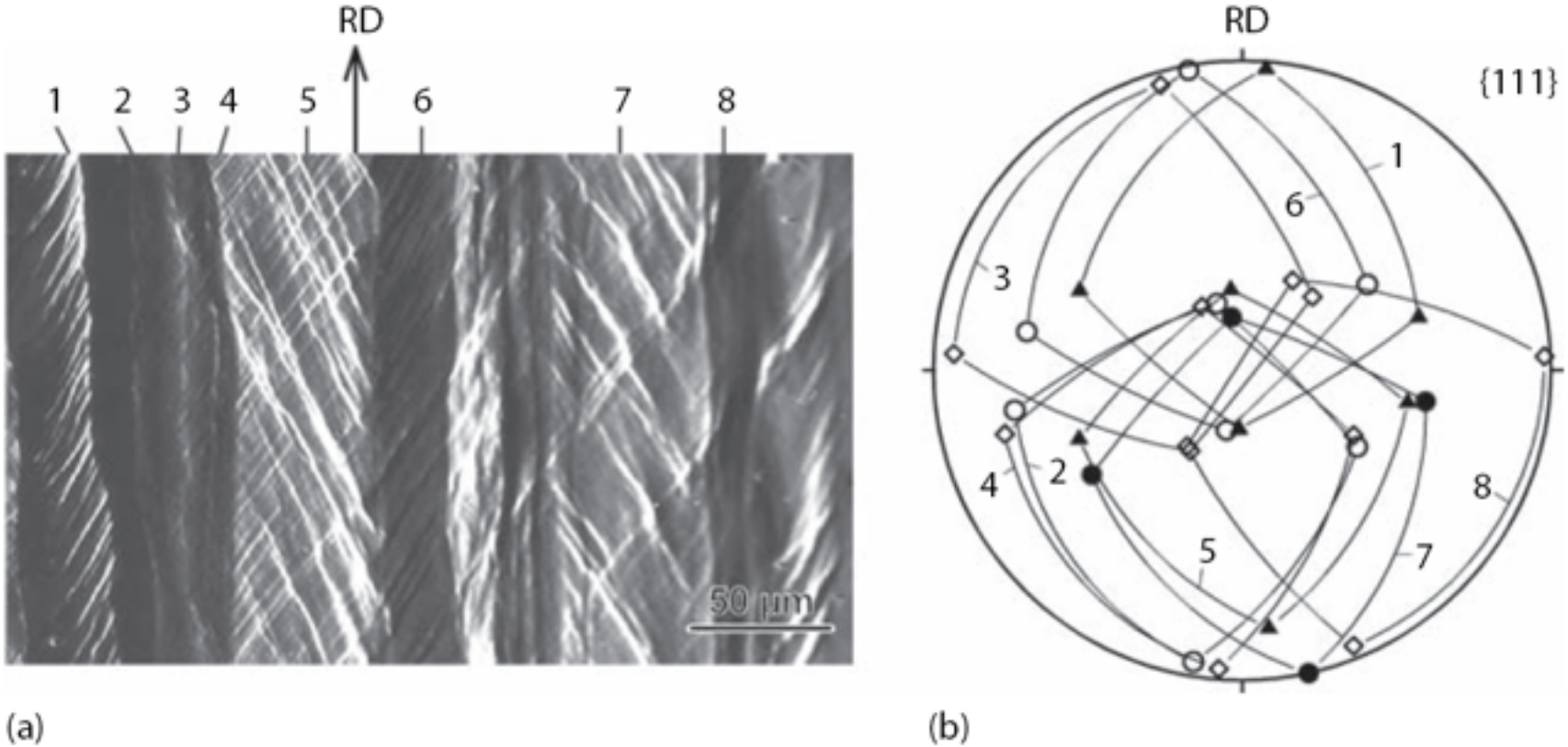

FIGURE 9.1
Example of the presentation of microtexture data in a pole figure, showing the influence of the matrix orientation on shear band formation in polycrystalline Al–3%Mg, 90% cold rolled. (a) Microstructure; (b) orientations of (a). Filled symbols—grains with shear bands; open symbols—grains without shear bands.

OP: individual orientation

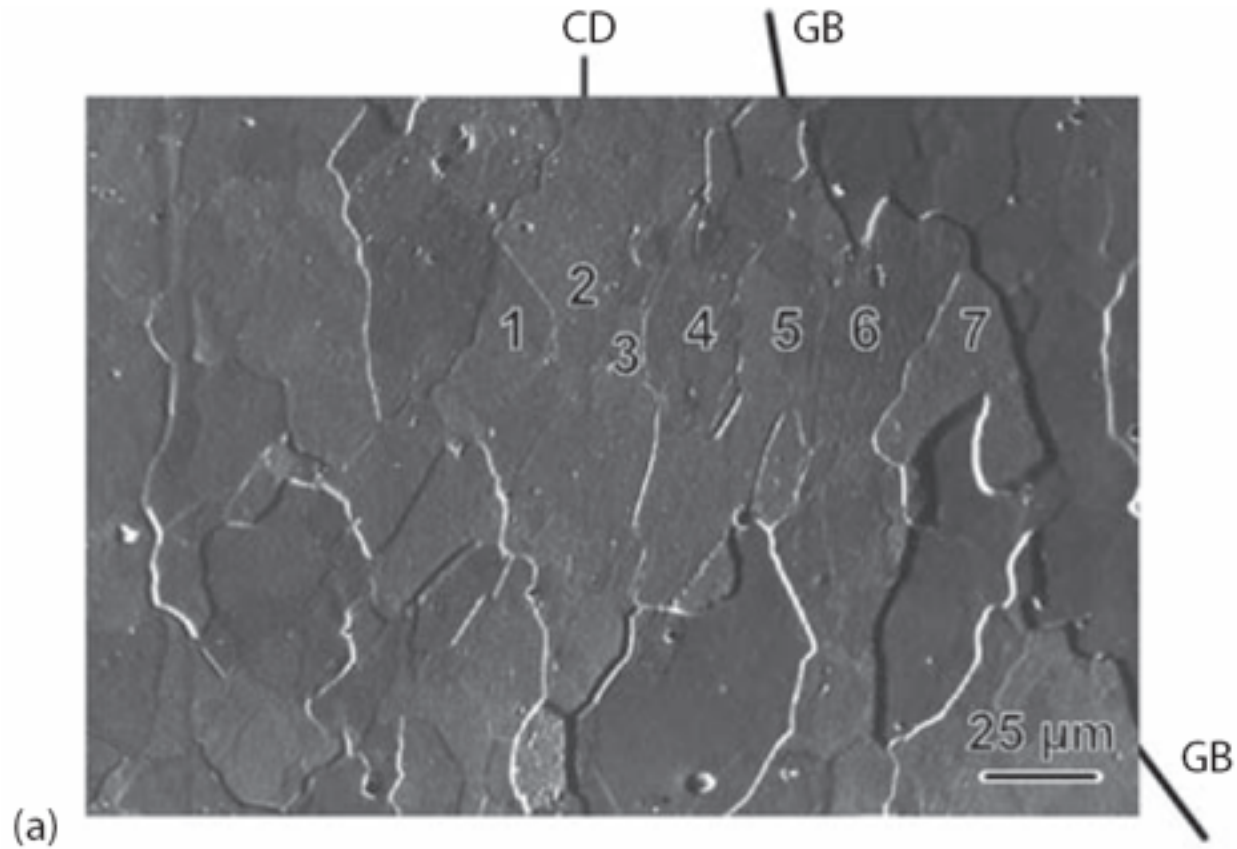

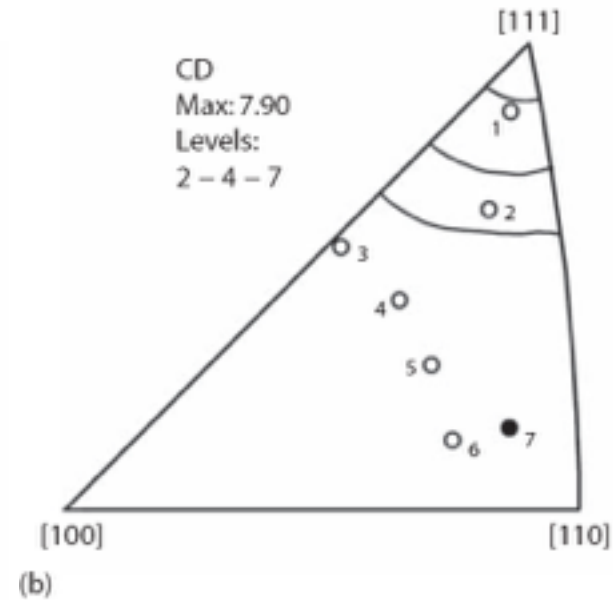

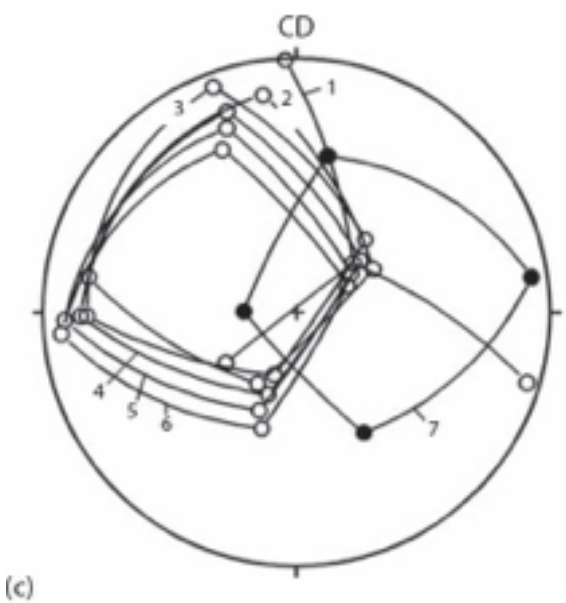

(a) Microstructure of NiAl deformed at 900°C by 70% in compression, showing a coarse subgrain structure in the vicinity of a grain boundary marked GB. (b) Inverse pole figure of the subgrain orientations shown in (a). The x-ray macrotexture of the sample mainly showed intensities close to [111], as indicated by the iso-intensity lines. EBSD single-grain orientation measurements of subgrains 1–7 close to the GB depict remarkable orientation changes. (c) Pole figure of the subgrain orientations 1–7 showing that the orientations of subgrains 6 and 7 were quite different. (Courtesy of L. Löchte and J. Fischer-Bühner.)

OP: density distribution

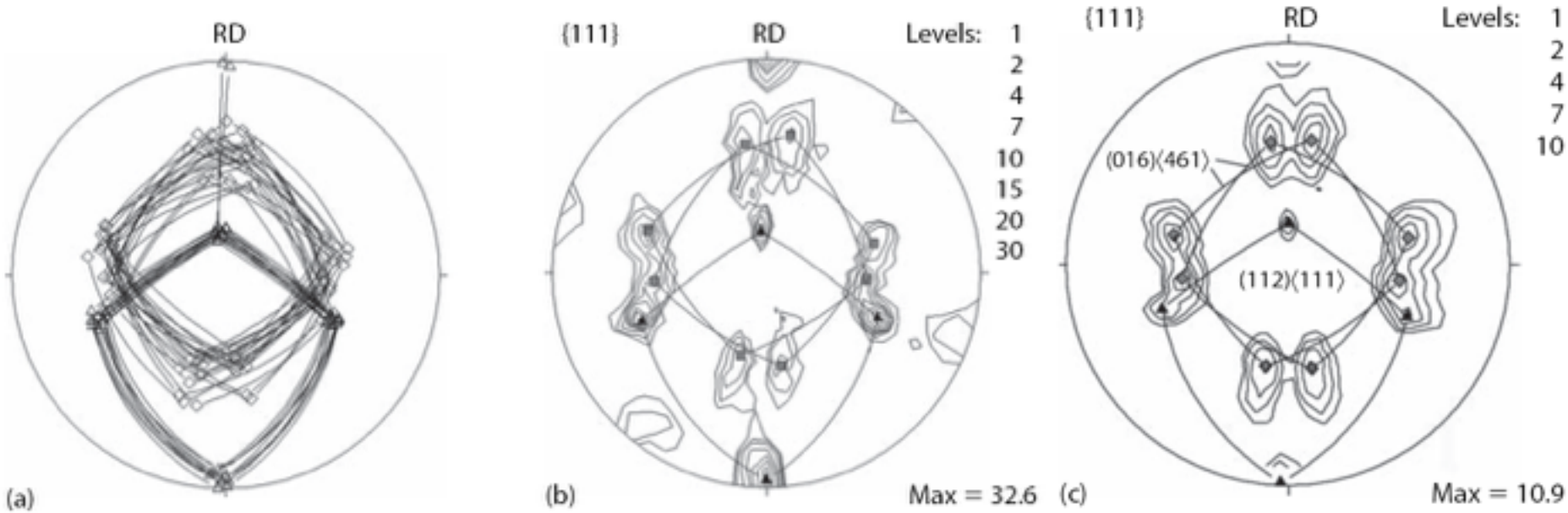

Def EBSD:
500 orientations

RX EBSD:
500 orientations

XRD

Comparison of EBSD microtexture and x-ray macrotexture pole figures of a partially recrystallized Al–1.8%Cu single crystal (rolled to 80% reduction, annealed for 300 s at 300°C). (a) Examples of EBSD single-grain orientation measurements in the as-deformed matrix and the new recrystallized grains; (b) continuous density distribution as computed from approximately 500 orientations similar as in (a); (c) x-ray macrotexture of the same sample.

$$\begin{pmatrix} \sin\alpha_i \cos\beta_i \\ \sin\alpha_i \sin\beta_i \\ \sin\alpha_i \end{pmatrix} = g^{-1} \cdot \begin{pmatrix} h_i \\ k_i \\ l_i \end{pmatrix}$$

OP: orientation smoothing

(a)

0.045	0.122	0.045
0.122	0.332	0.122
0.045	0.122	0.045

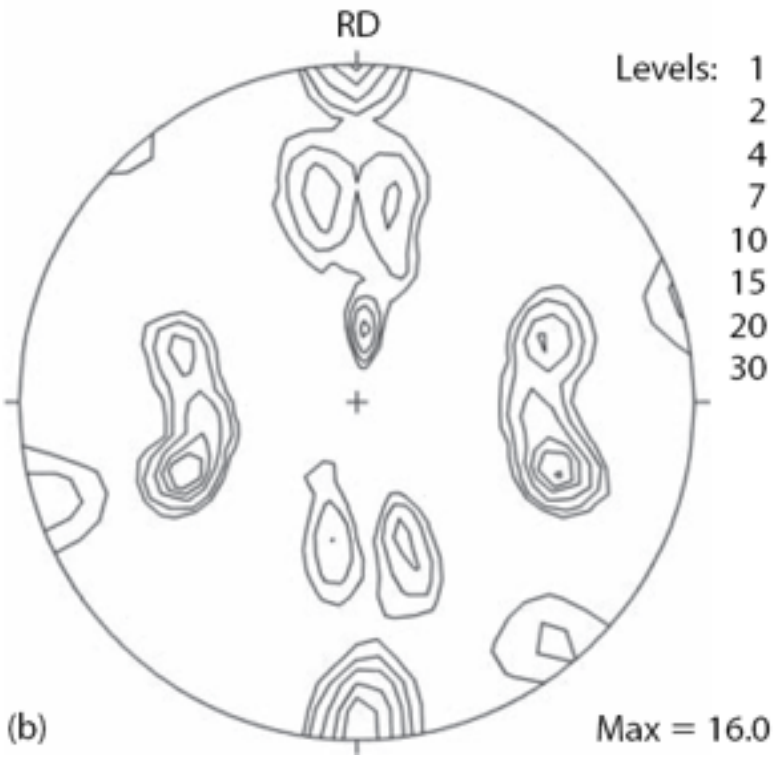

2D filter with an Gauss-shape

Smoothing of pole figure data. (a) Two-dimensional filter with approximate Gauss-shape to smooth pole figures; (b) pole figure as derived from pole figure data as in Figure 9.3c but smoothed with the filter in (a).

Euler space: individual orientations

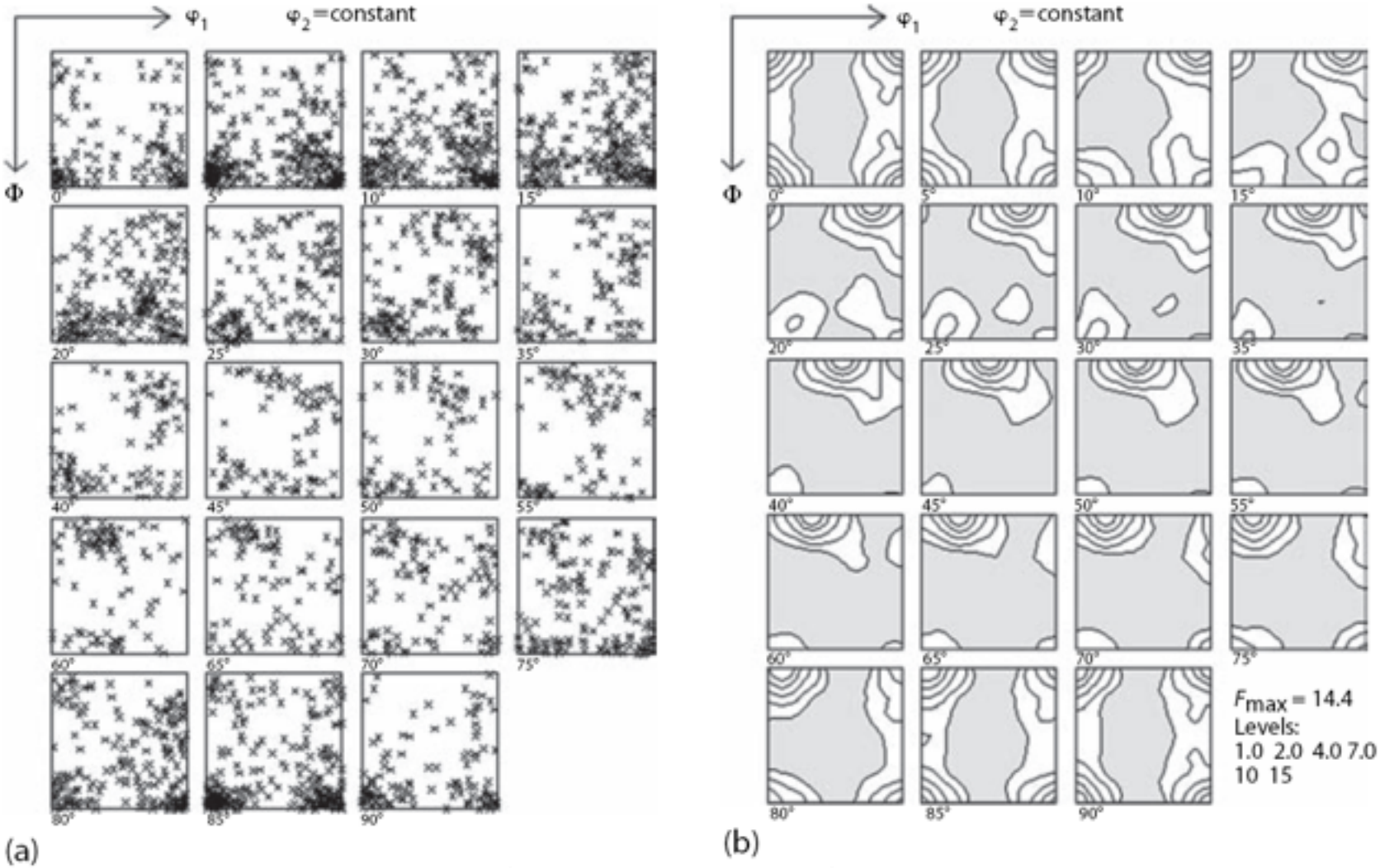

Presentation in Euler space of microtexture data of a recrystallized aluminum sample. (a) Orientations of 1000 grains as obtained by EBSD; (b) continuous intensity function (ODF) as derived from x-ray pole figure measurements of the same sample, showing good reproducibility of the main texture features.

Euler space: individual orientations

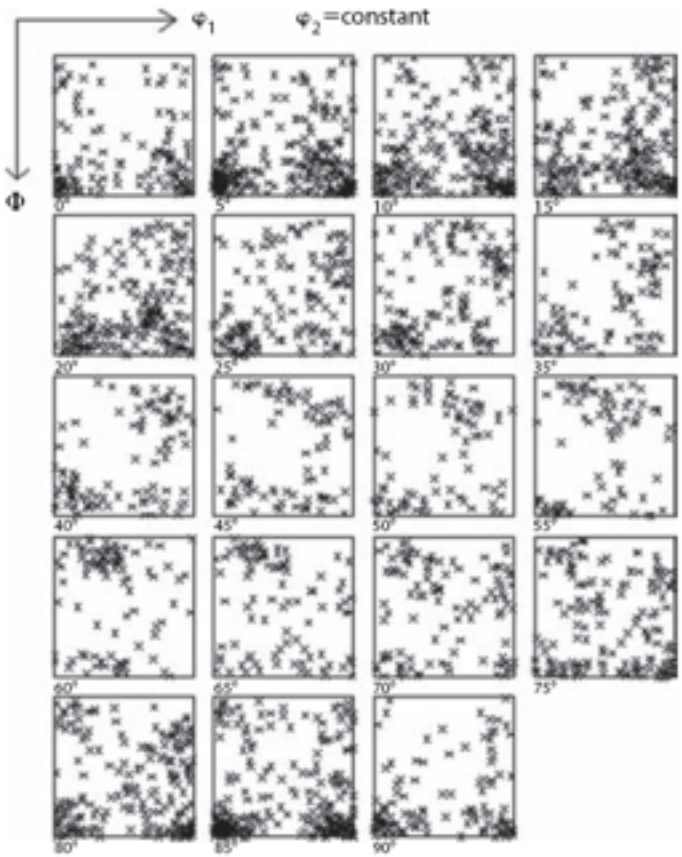

(a)

After reduction with regard to sample and crystal symmetry, orientations don't fall exactly in one of the sections. This resulting error can slightly be reduced by projecting orientations under $\Phi = 0$ = constant for $\varphi_1 + \varphi_2$.

Each individual orientation has to appear three times in the space, because the threefold axis of cubic crystal symmetry is not considered.

Presentation in Euler space of microtexture data of a recrystallized aluminum sample. (a) Orientations of 1000 grains as obtained by EBSD; (b) continuous intensity function (ODF) as derived from x-ray pole figure measurements of the same sample, showing good reproducibility of the main texture features.

Euler space: continuous distribution

$$S(\Psi) = S_0 \cdot \exp\left[-\left(\frac{\Psi}{\Psi_0}\right)^2\right]$$

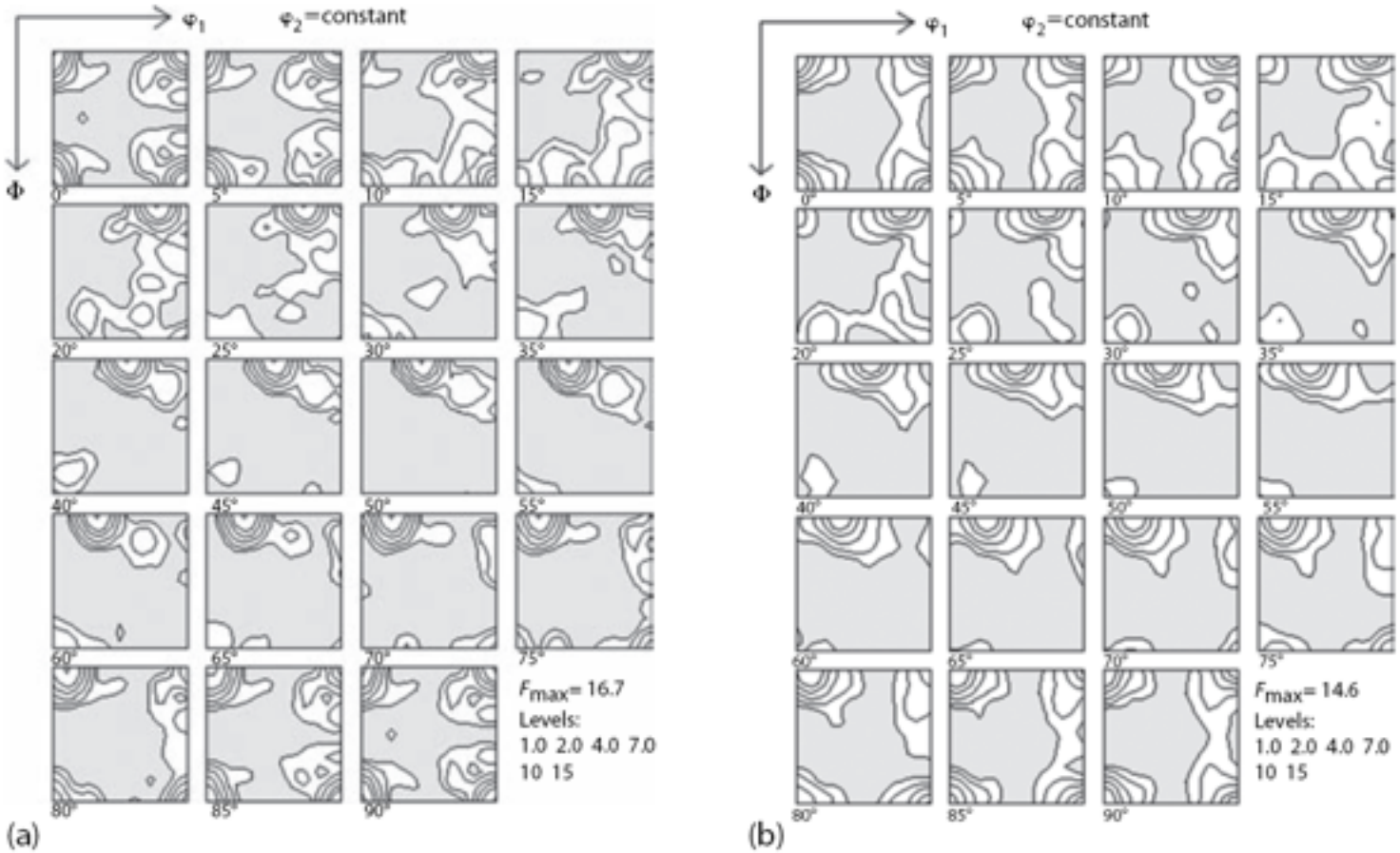

ODFs of recrystallized aluminum, as in Figure 9.5, calculated from different numbers N of EBSD single-grain orientation measurements, (a) $N = 100$, (b) $N = 1000$.

Euler space: statistic relevance

Bunge 1982 states that for ODF determination with statistic relevance (80% reliability) 25 points per cell are necessary. For ODF 90 x 90x 90 and a cell size of 5, this require 10,000 orientation measurement.

For cubic materials, only 100 orientations is needed to comprise the main characteristic textures, whereas 500-1000 orientations are required to obtain a statistically sound texture distribution.

The statistic parameter

$$\rho_{0,N} = \frac{\oint (f_0 - f_N)^2 dg}{\oint f_0^{\,2} dg} \cdot 100\%$$

Reference ODF

N'=300 N=400

$$\rho_{N',N} = \frac{\oint (f_{N'} - f_N)^2 dg}{\oint f_N^{\,2} dg} \cdot 100\%$$

Statistical parameter

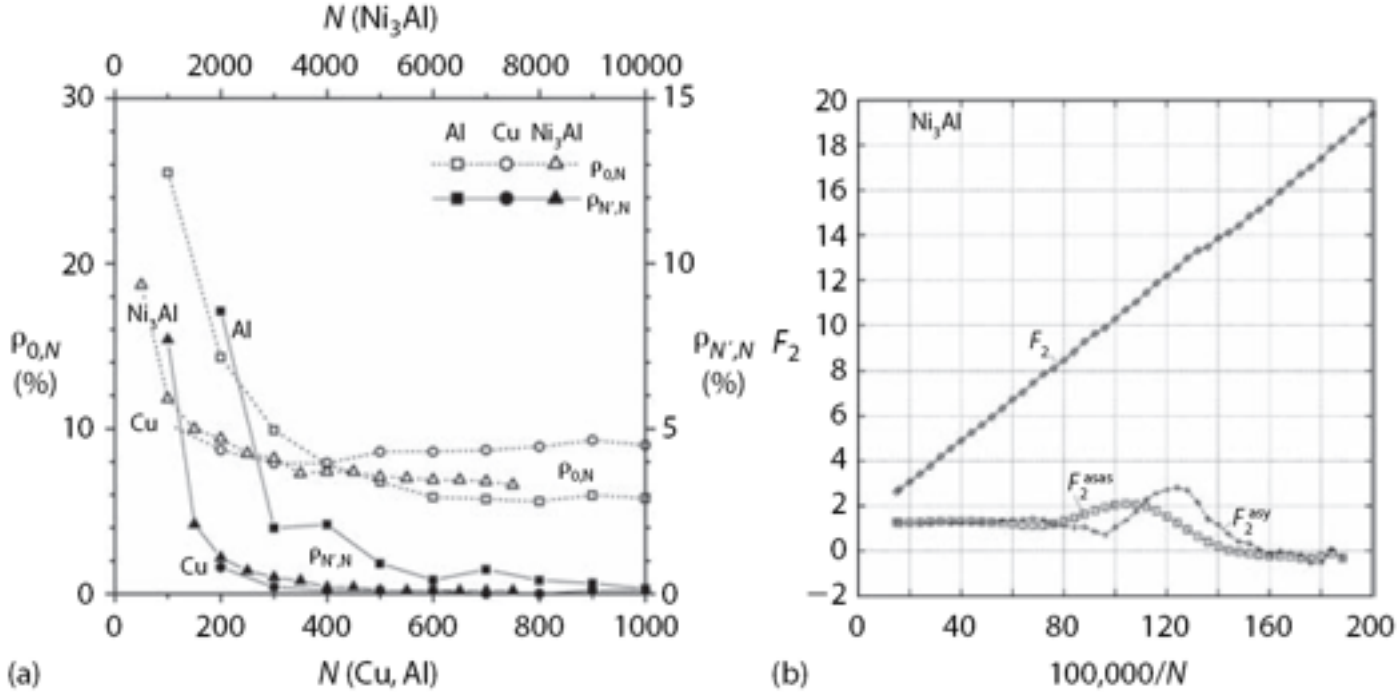

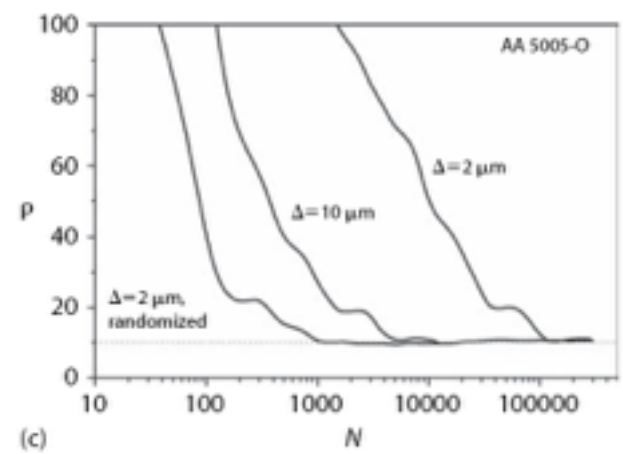

Statistical assessment of single-grain orientation measurements. Evolution of (a) the statistical parameters $\rho_{0,N}$ and $\rho_{N',N}$ with increasing number of single-grain orientation measurements N for different texture examples, (b) F_2 with $1/N$ for recrystallized Ni_3Al, and (c) $\rho_{0,N}$ with N for different scanning procedures in recrystallized Al–Mg.

Misorientation analysis: Grain boundaries

3D Rodrigues space

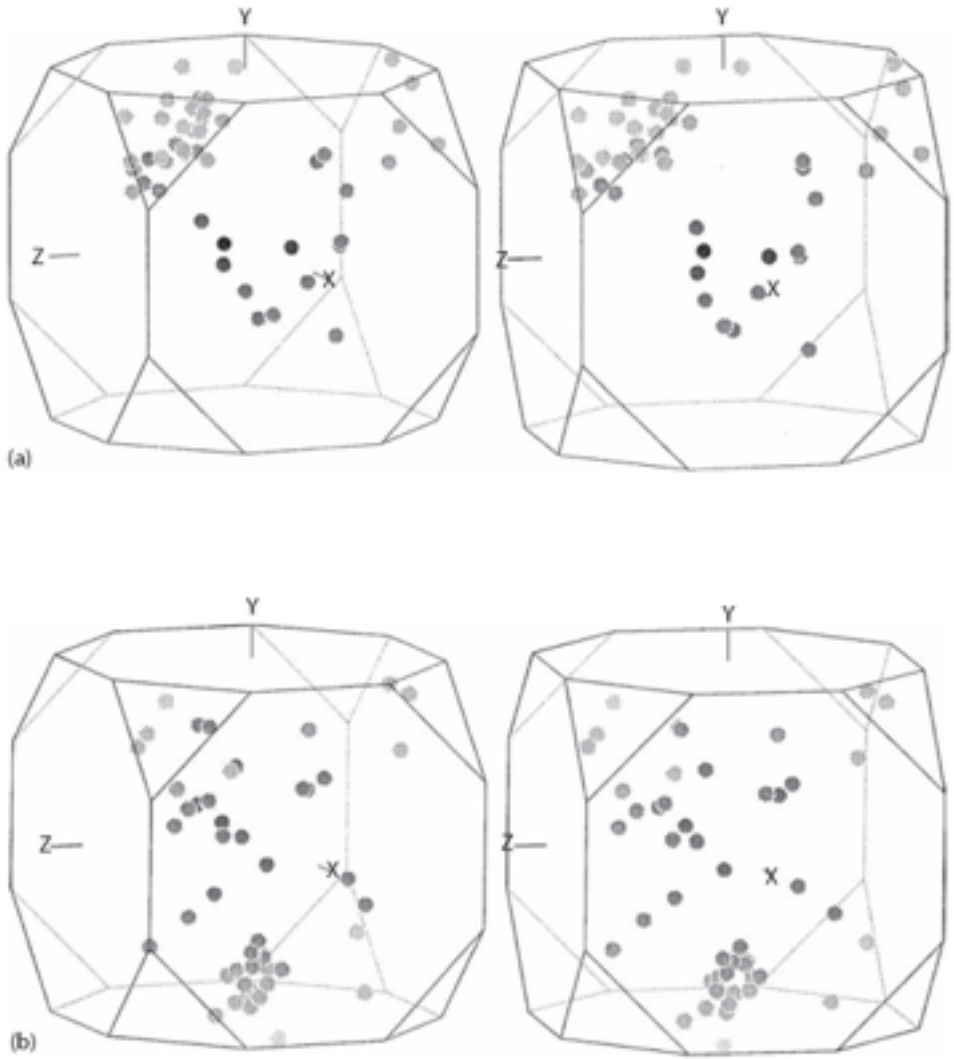

Textures from an aluminum–lithium alloy displayed in Rodrigues space as stereo pairs. Data sets are of 50 grains having (a) predominantly *S*1 orientation and (b) predominantly *S*2 orientation. (Adapted from Randle, V. and Day, A., *Mater. Sci. Technol.*, 9, 1069, 1993.)

Rodrigues space Z-axis perspective view

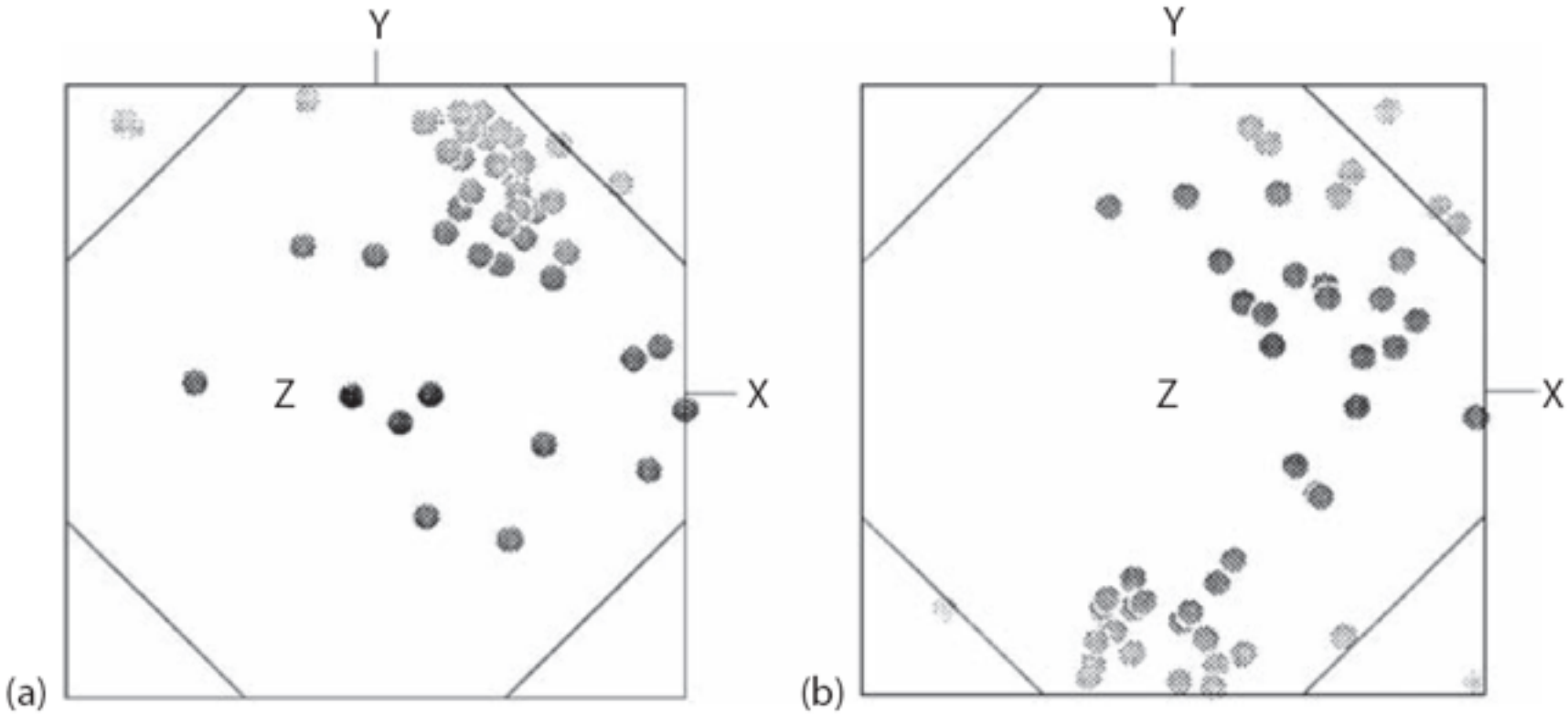

Rodrigues space Z-axis perspective view of the microtextures in Figures 9.8a and 9.8b, respectively. (Adapted from Randle, V. and Day, A., *Mater. Sci. Technol.*, 9, 1069, 1993.)

Fiber texture in Rodrigues space

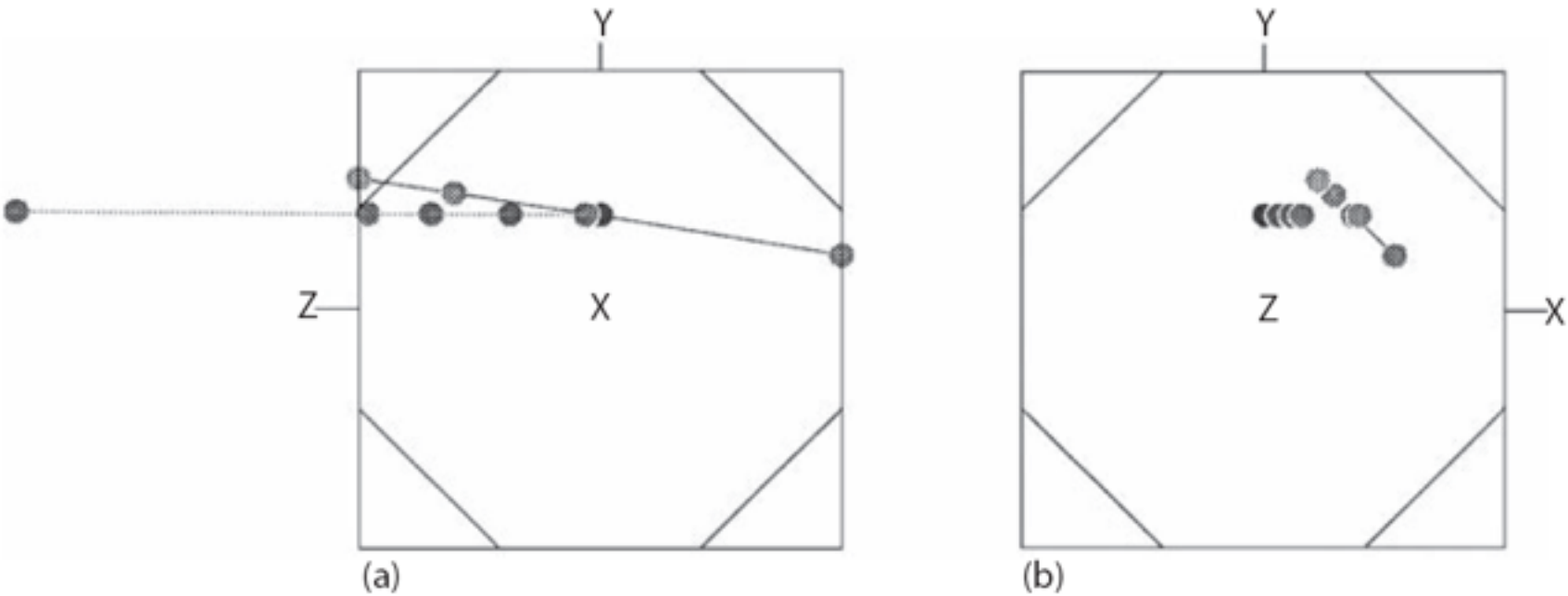

{103}<hkl> {103}<hkl>

Fiber textures in Rodrigues space for {103}⟨*hkl*⟩ (dotted line) and {$\bar{1}$13}⟨*hkl*⟩ (dashed line). Both (a) the X-axis perspective and (b) the Z-axis perspective are shown. (Adapted from Randle, V. and Day, A., *Mater. Sci. Technol.*, 9, 1069, 1993.)

Components of Rodrigues space

uvw	R_1	R_2	R_3
001 fiber axis			
100	0	0	0
$3\bar{1}0$	0	0	0.162
$2\bar{1}0$	0	0	0.236
$3\bar{2}0$	0	0	0.303
$1\bar{1}0$	0	0	0.414
$\bar{1}01$ fiber axis			
101	0	0.414	0
212	0.071	0.414	−0.172
111	0.132	0.414	−0.318
121	0.214	0.414	−0.518
131	0.263	0.414	−0.634
$\bar{1}11$ fiber axis			
$1\bar{1}2$	0.214	0.518	0.414
101	0.318	0.414	0.132
312	0.379	0.353	−0.036
211	0.414	0.318	−0.132
110	0.518	0.214	−0.414
103 fiber axis			
010	0.162	0.162	1
$33\bar{1}$	0.065	0.162	0.399
$32\bar{1}$	0.047	0.162	0.290
$31\bar{1}$	0.025	0.162	0.154
301	0	0.162	0
$\bar{1}13$ fiber axis			
$3\bar{3}2$	0.093	0.224	0.414
$2\bar{1}1$	0.119	0.198	0.251
301	0.154	0.162	0.025
110	0.224	0.093	−0.414

Source: Data from Randle, V. and Day, A., *Mater. Sci. Technol.*, 9, 1069, 1993.

Orientation distribution in Rodrigues space

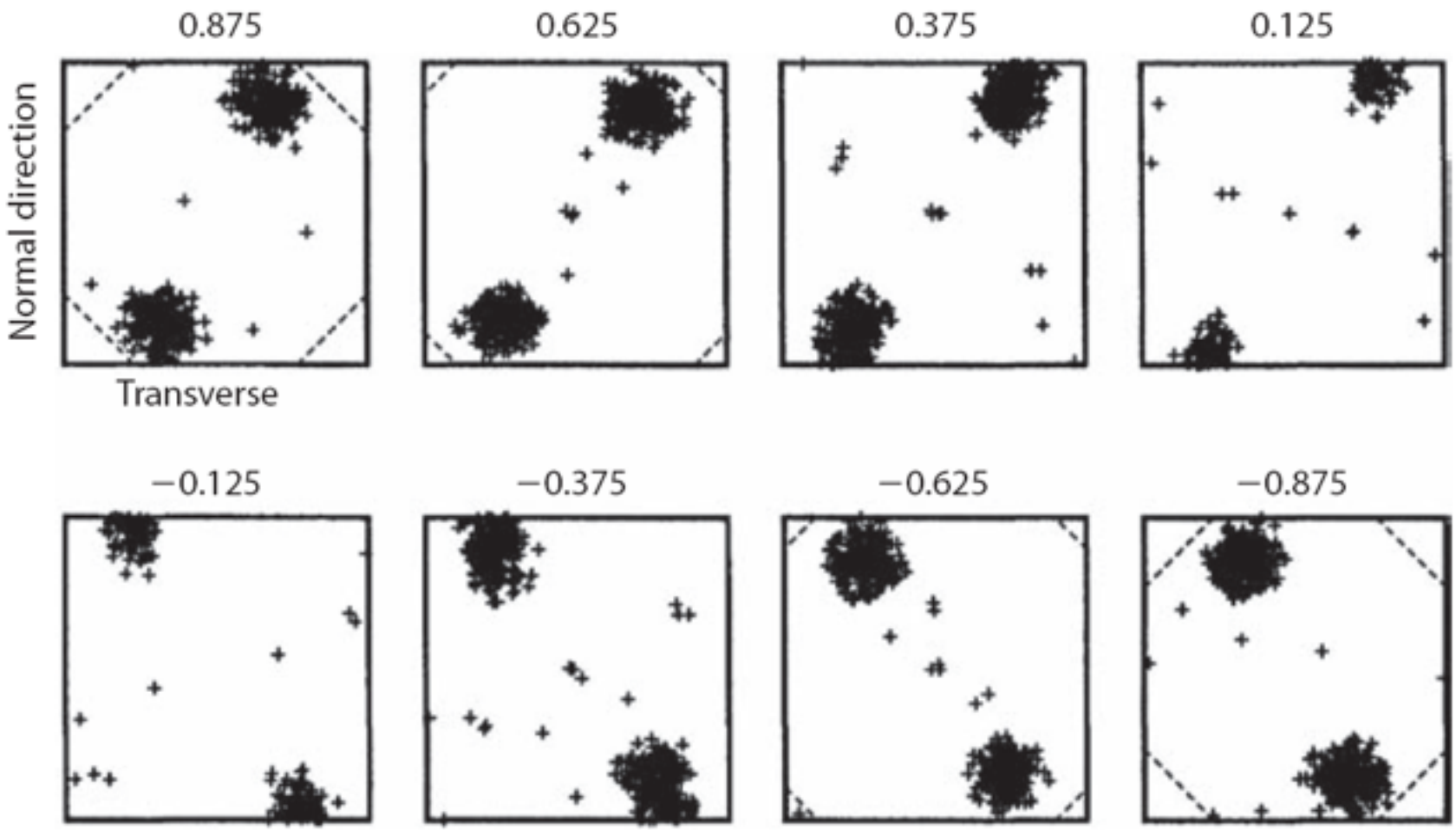

Example of orientation distributions in Rodrigues space displayed as sections in R_3: copper rolling texture and cubic symmetry. (Data from Becker, R. and Panchanadeeswaran, S., *Text. Microstruct.*, 10, 167, 1989.)

Representation of Misorientation: angle/axis

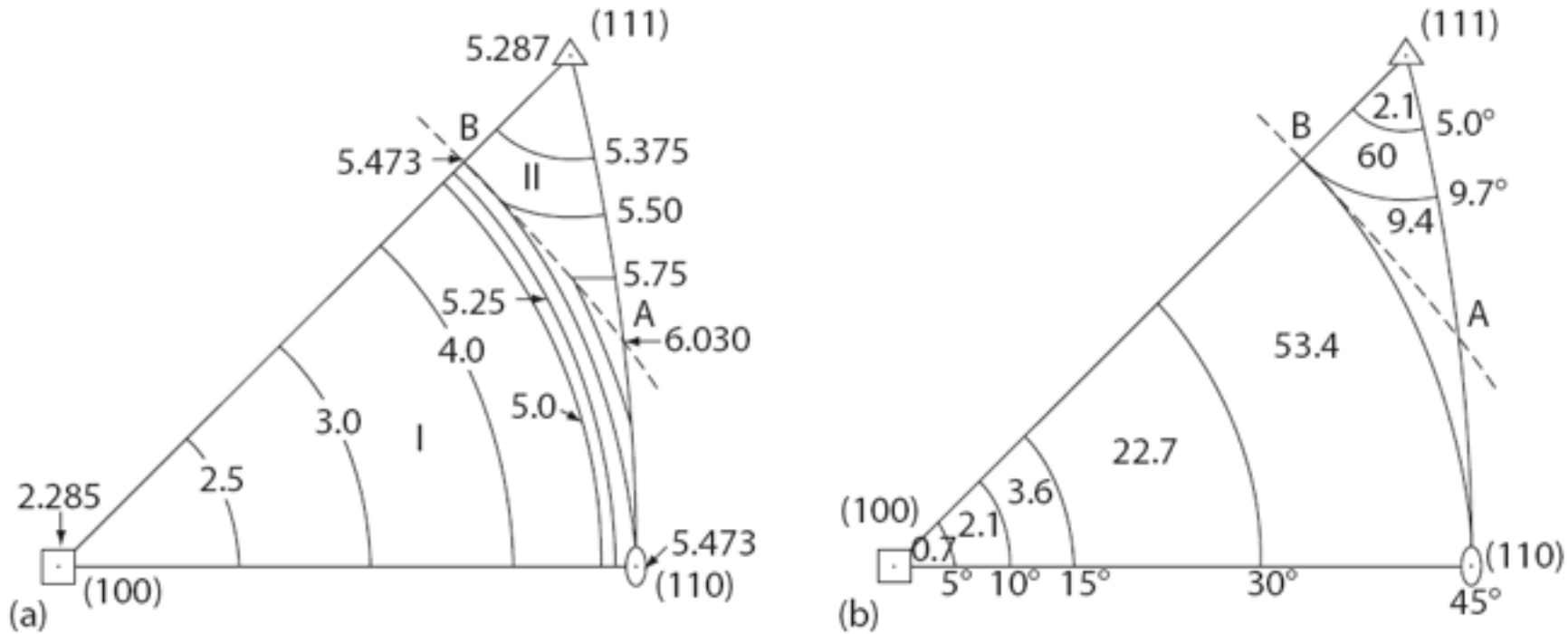

Distribution of disorientation axes [*hkl*] for cubic crystals in a single unit triangle of the stereographic projection. (a) Probability density plot; (b) percentage of disorientation axes lying in the various regions. (Data from Mackenzie, J.K., *Acta Metall.*, 12, 223, 1964.)

Disorientation axis distribution

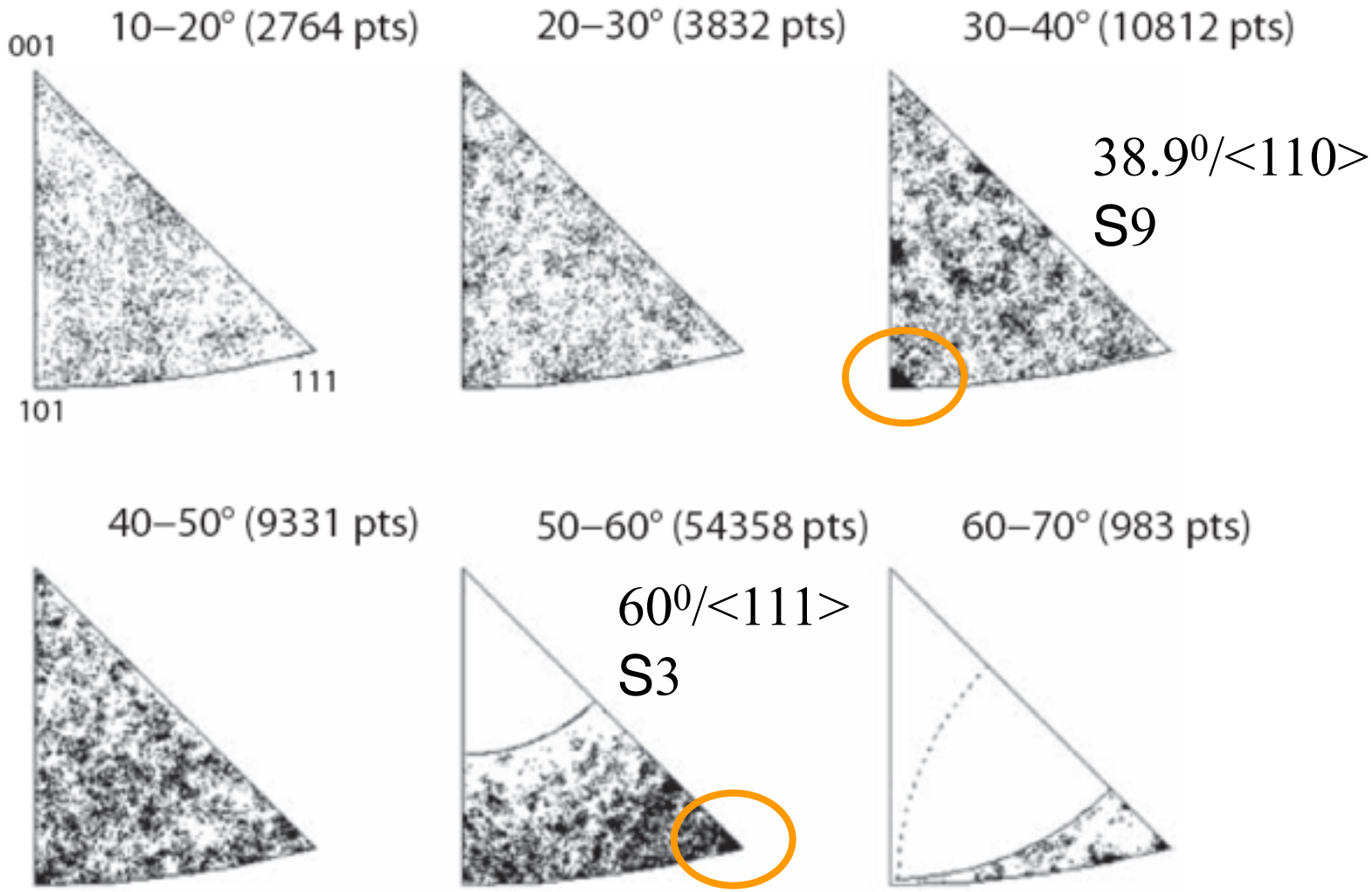

For Cu with 10° angle sections

Disorientation angle distribution

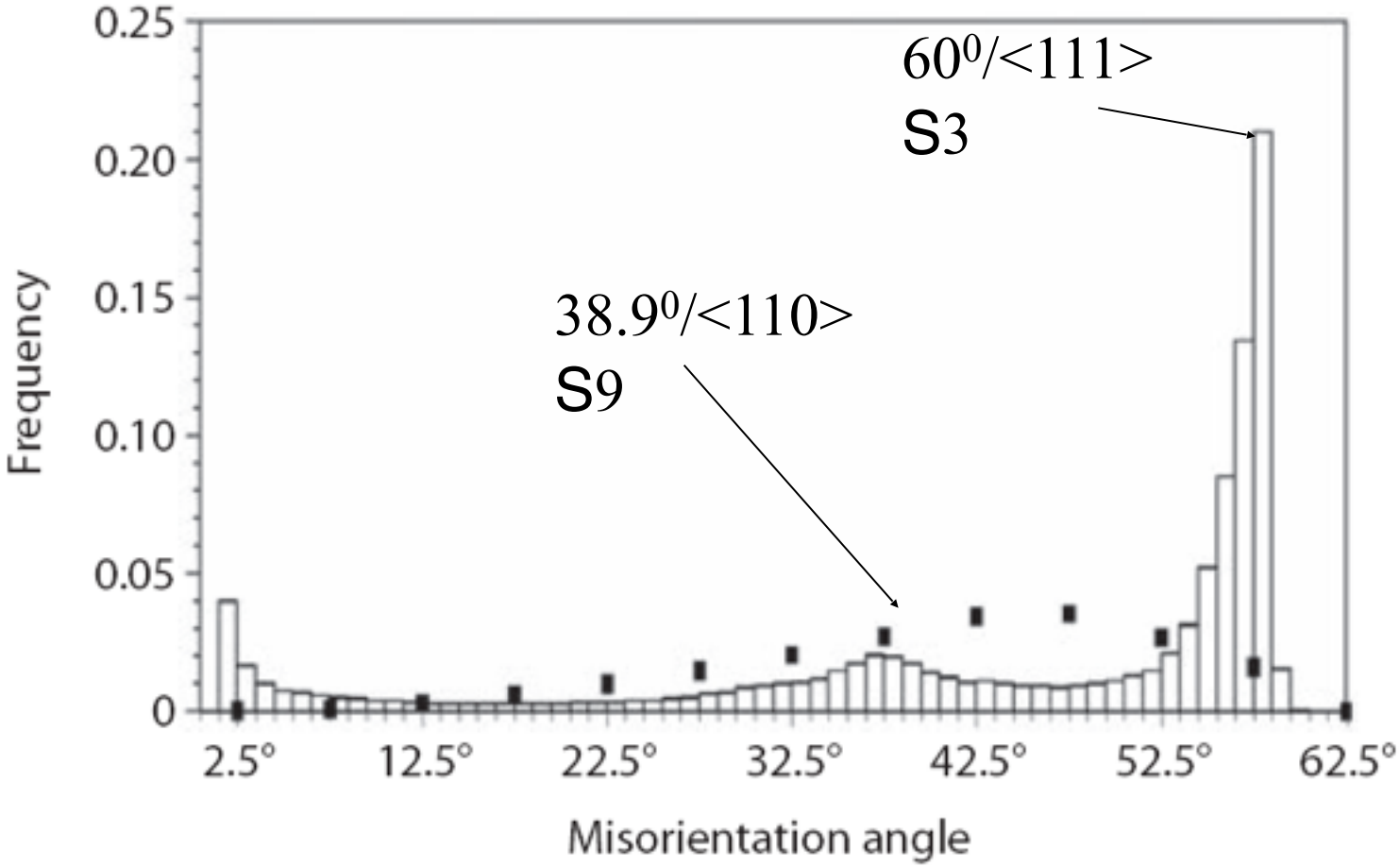

Distribution of disorientation angles for copper; same data set as in Figure 9.13. The distribution for randomly misoriented crystal pairs that have cubic symmetry (the "Mackenzie distribution") is also included.

Correlated and uncorrelated misorientation

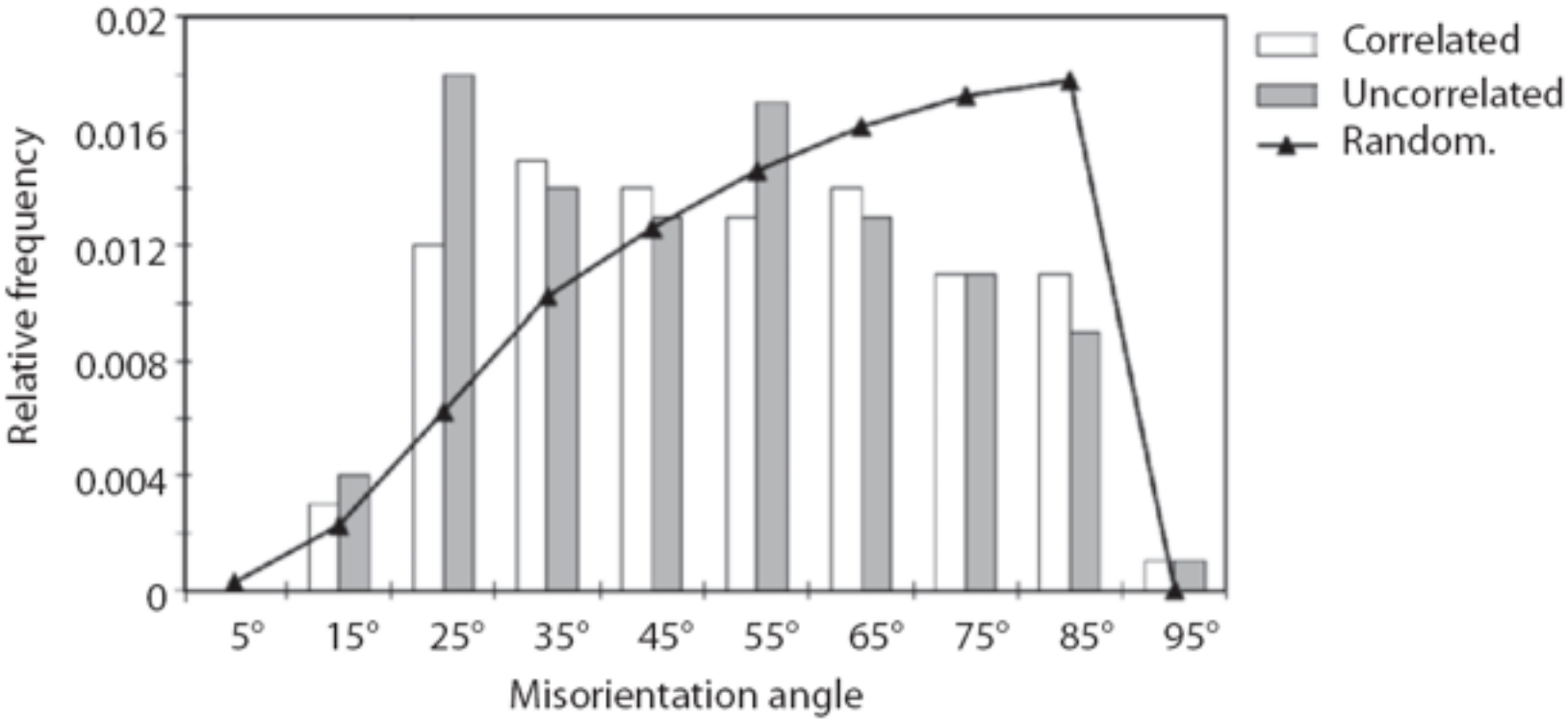

Disorientation angle distribution histogram for correlated and uncorrelated misorientation pairs in commercially pure titanium. The disorientation angle distribution for randomly misoriented crystal pairs is also included (with triangles).

Random distribution

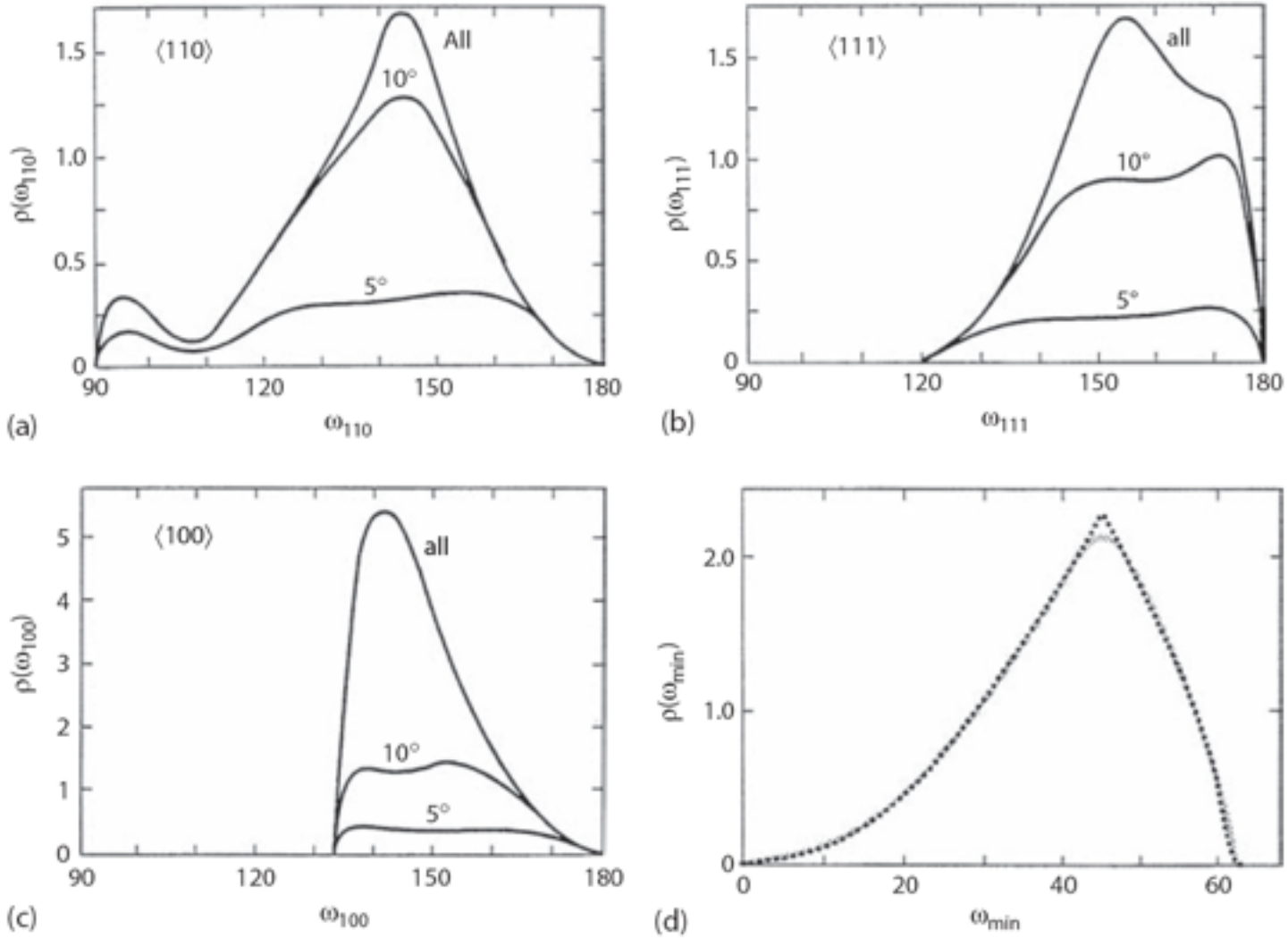

Distributions of computer-generated misorientation angles for a random distribution plotted for misorientation axes closest to (a) ⟨110⟩, (b) ⟨111⟩, (c) ⟨100⟩, and (d) disorientation axes. (Courtesy of W.B. Hutchinson.)

Misorientation ODF in Euler space

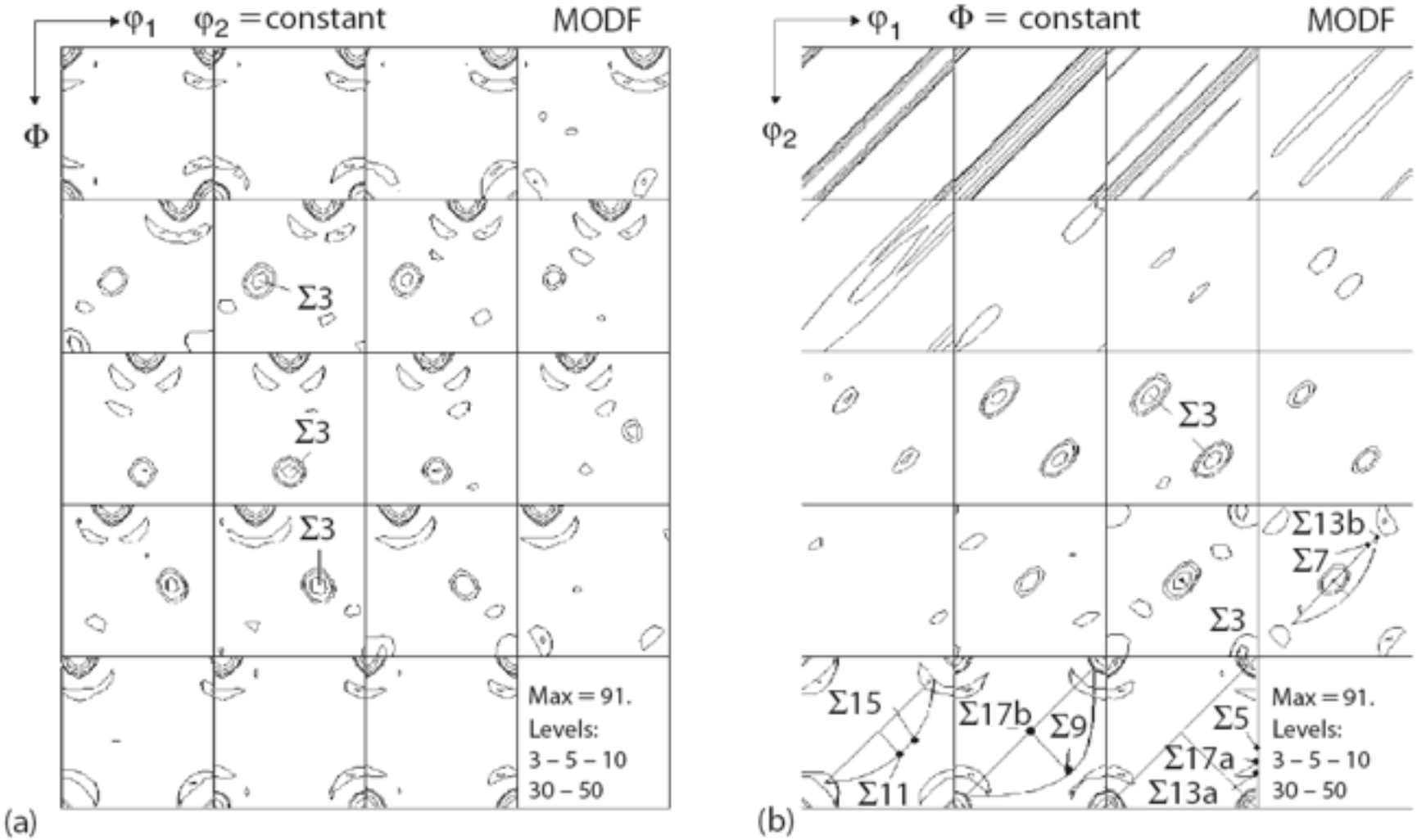

Representation of the MODF of a cyclically deformed nickel specimen in Euler space. (a) φ_2 = constant; (b) Φ = constant.

MODF in cylindrical angle/axis space

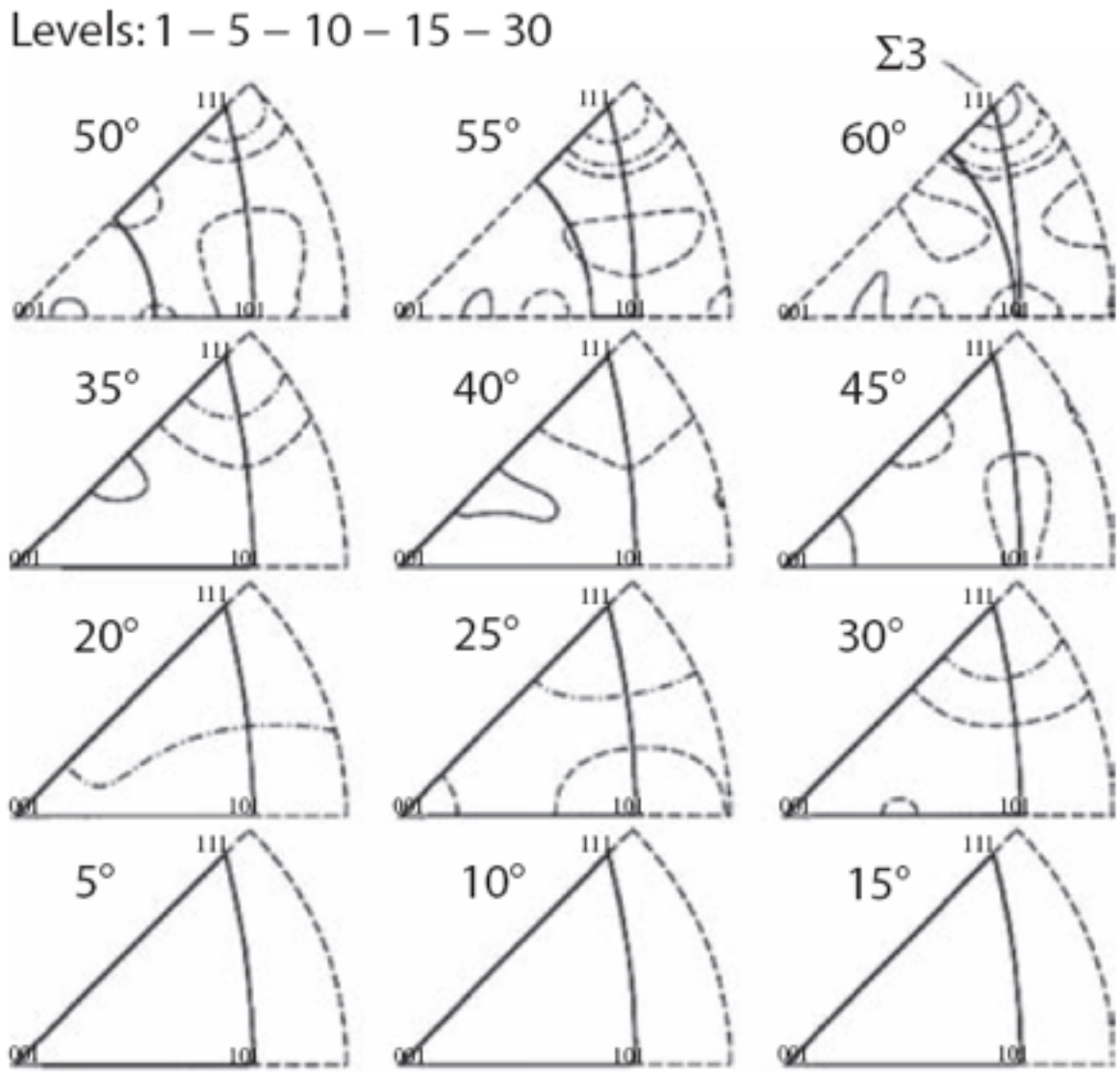

For deformed Ni

MODF in Rodrigues space

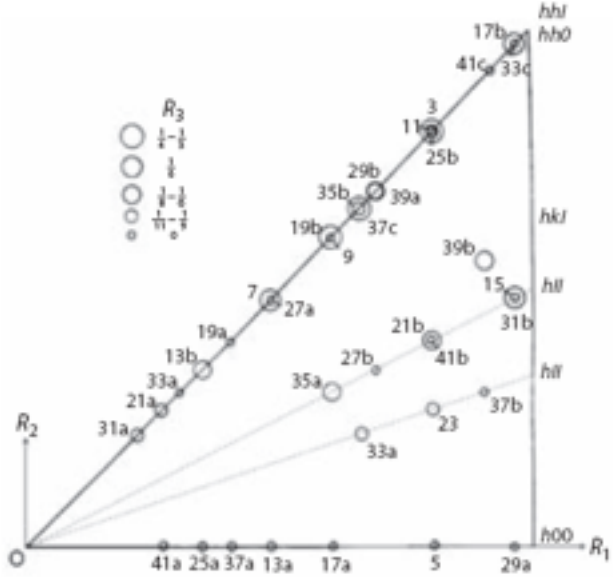

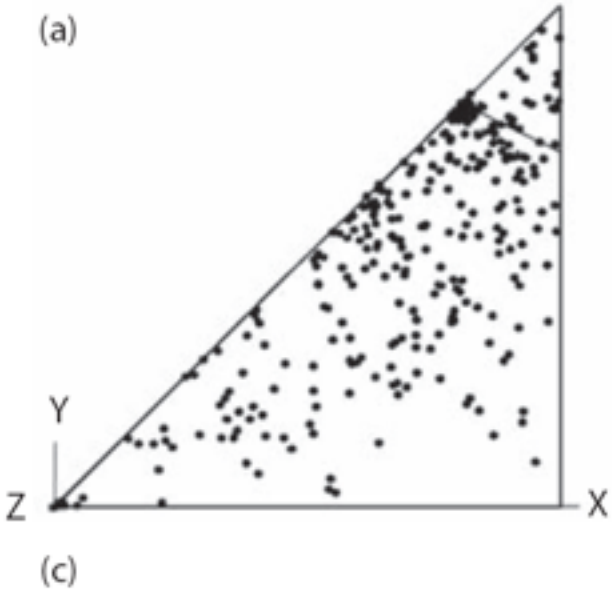

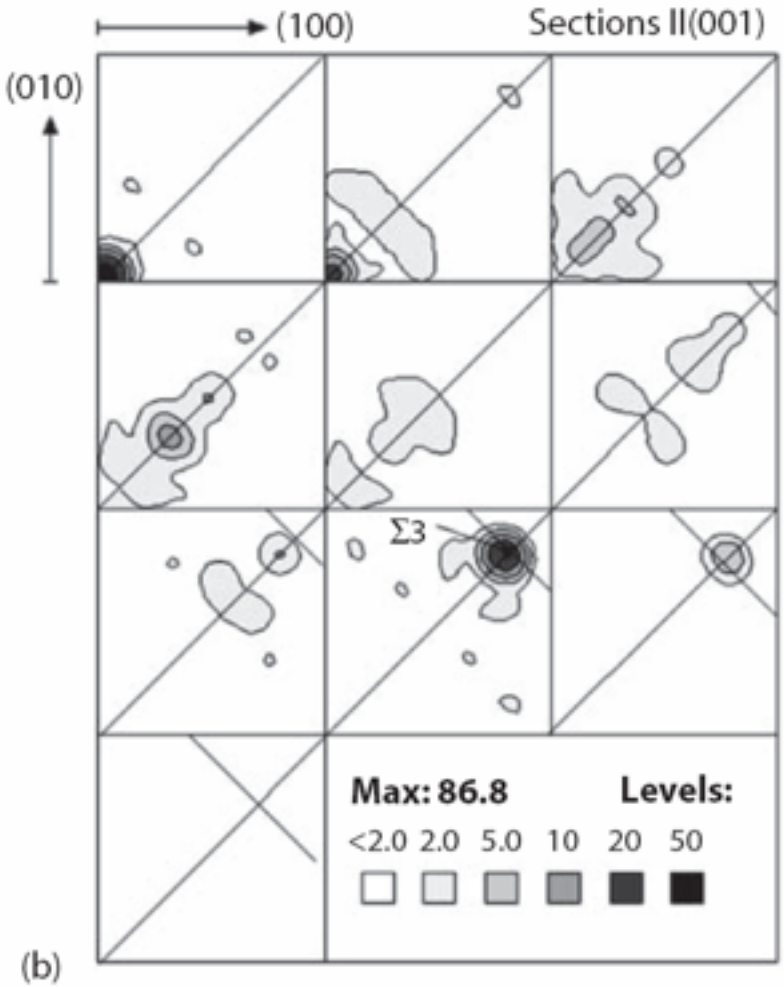

For CSLs

Rodrigues Vectors for CSLs

Rodrigues Vectors for CSLs up to $\Sigma = 45$

Axis/Σ	R_1	R_2	R_3
⟨100⟩			
5	1/3	0	0
13a	1/5	0	0
17a	1/4	0	0
25a	1/7	0	0
29a	2/5	0	0
37a	1/6	0	0
41a	1/9	0	0
⟨210⟩			
15	2/5	1/5	0
27b	2/7	1/7	0
41b	2/6	1/6	0
43b	2/9	1/9	0
⟨311⟩			
23	3/9	1/9	1/9
33b	3/11	1/11	1/11
⟨111⟩			
3	1/3	1/3	1/3
7	1/5	1/5	1/5
13b	1/7	1/7	1/7
19b	1/4	1/4	1/4
21a	1/9	1/9	1/9
31a	1/11	1/11	1/11
37c	3/11	3/11	3/11
39a	1/6	1/6	1/6
43a	1/13	1/13	1/13
⟨310⟩			
37b	3/8	1/8	0
⟨321⟩			
39b	3/8	2/8	1/8
⟨110⟩			
9	1/4	1/4	0
11	1/3	1/3	0
19a	1/6	1/6	0
27a	1/5	1/5	0
33a	1/8	18	0
33c	2/5	2/5	0
41c	3/8	3/8	0
⟨211⟩			
21b	2/6	1/6	1/6
31b	2/5	1/5	1/5
35a	2/8	1/8	1/8
⟨221⟩			
17b	2/5	2/5	1/5
29b	2/7	2/7	1/7
45b	2/9	2/9	1/9
45c	2/6	2/6	1/6
⟨331⟩			
25b	3/9	3/9	1/9
35b	3/11	3/11	1/11
⟨332⟩			
43c	3/8	3/8	2/8

Components of Rodrigues space

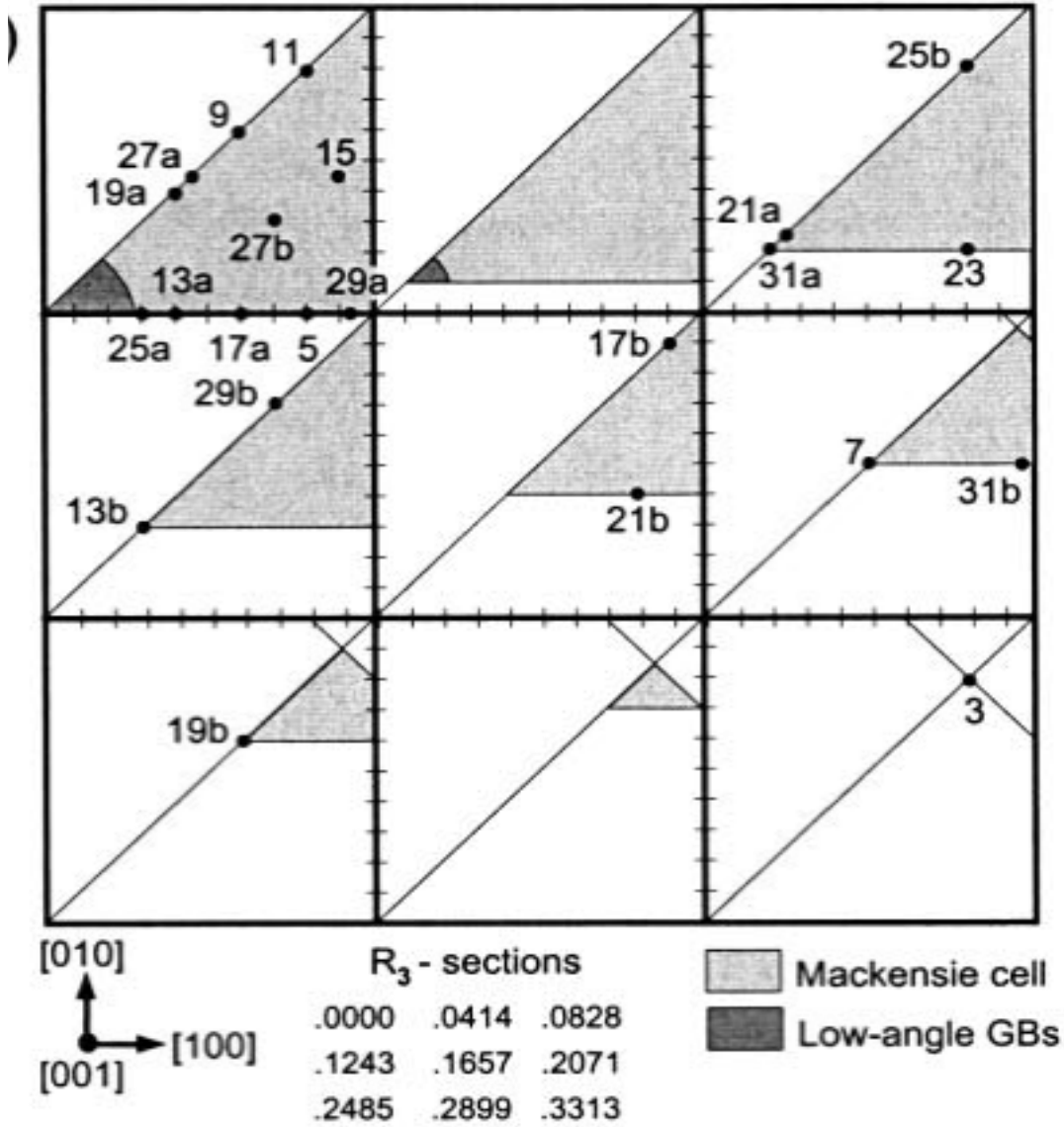

MODF, ODDF and OCF

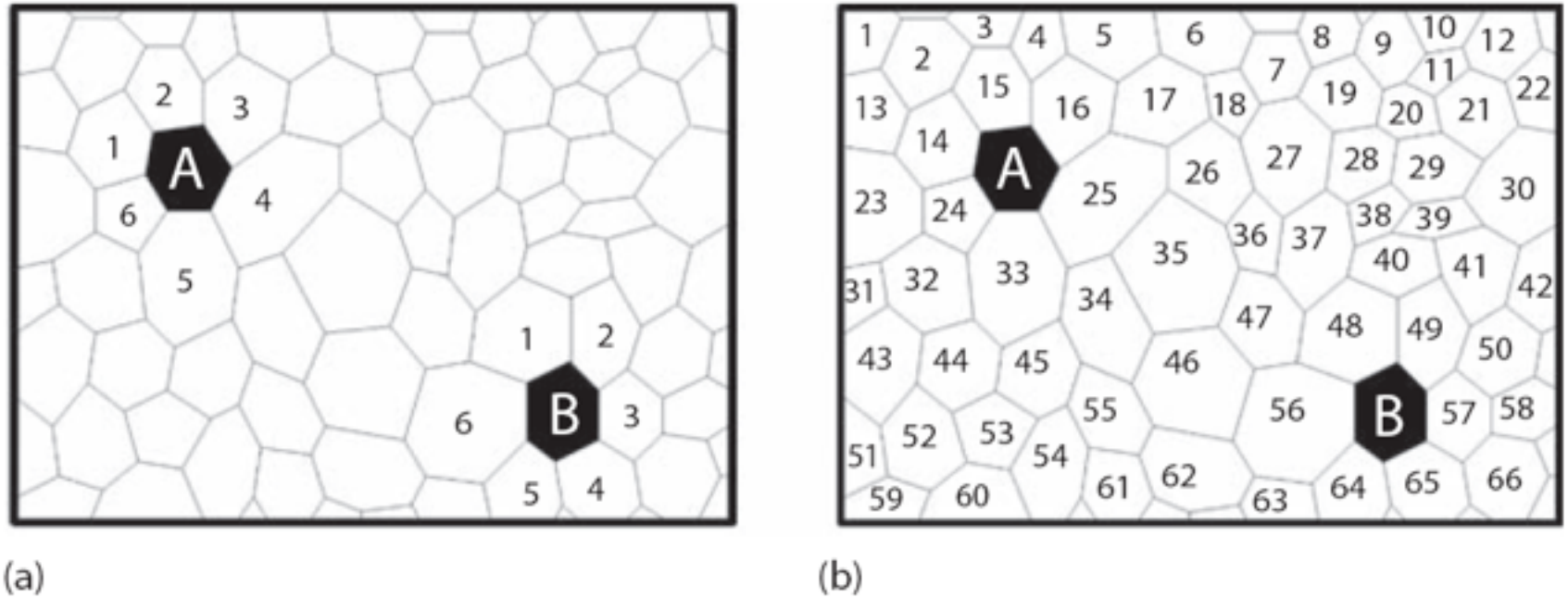

MODF: misorientations between grain i and all direct neighbors j

ODDF: misorientation between all grains i and j

OCF: orientation correlation function (texture-reduced spatial correlation of misorientations)

ODF and ODDF

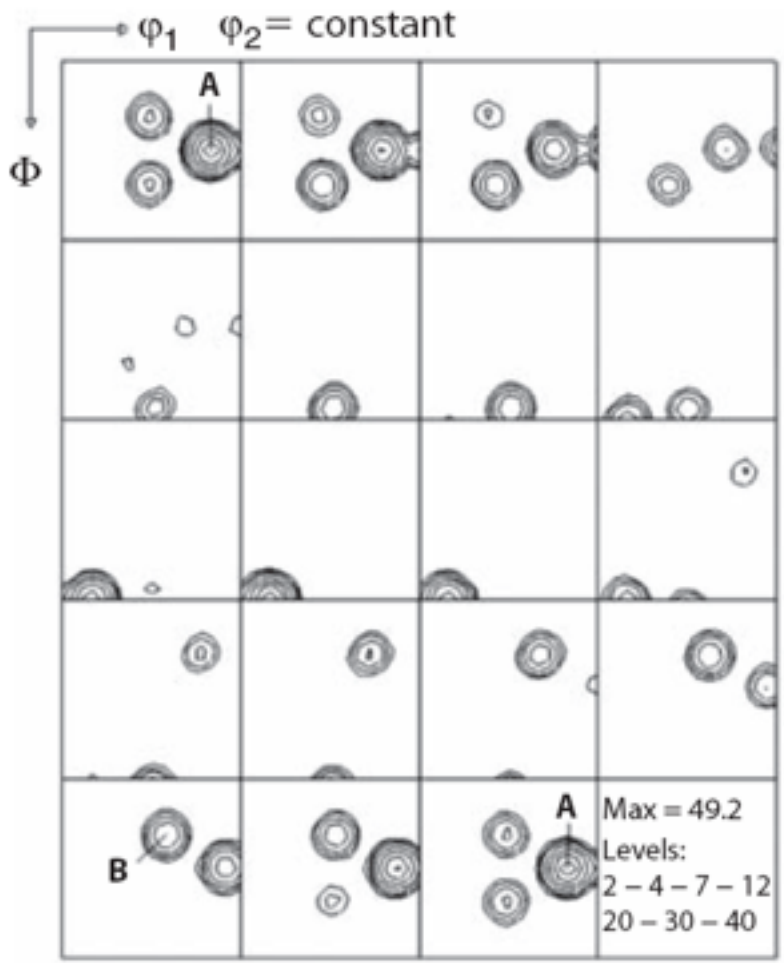

(a)

ODF

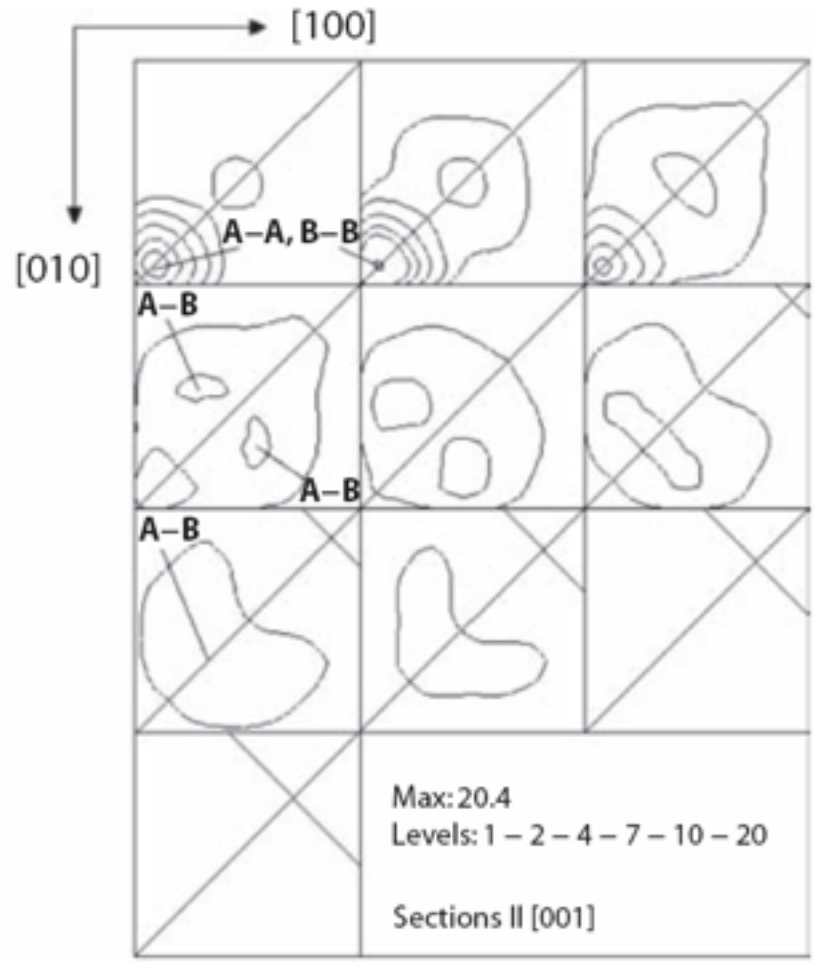

(b)

ODDF

MODF and OCF

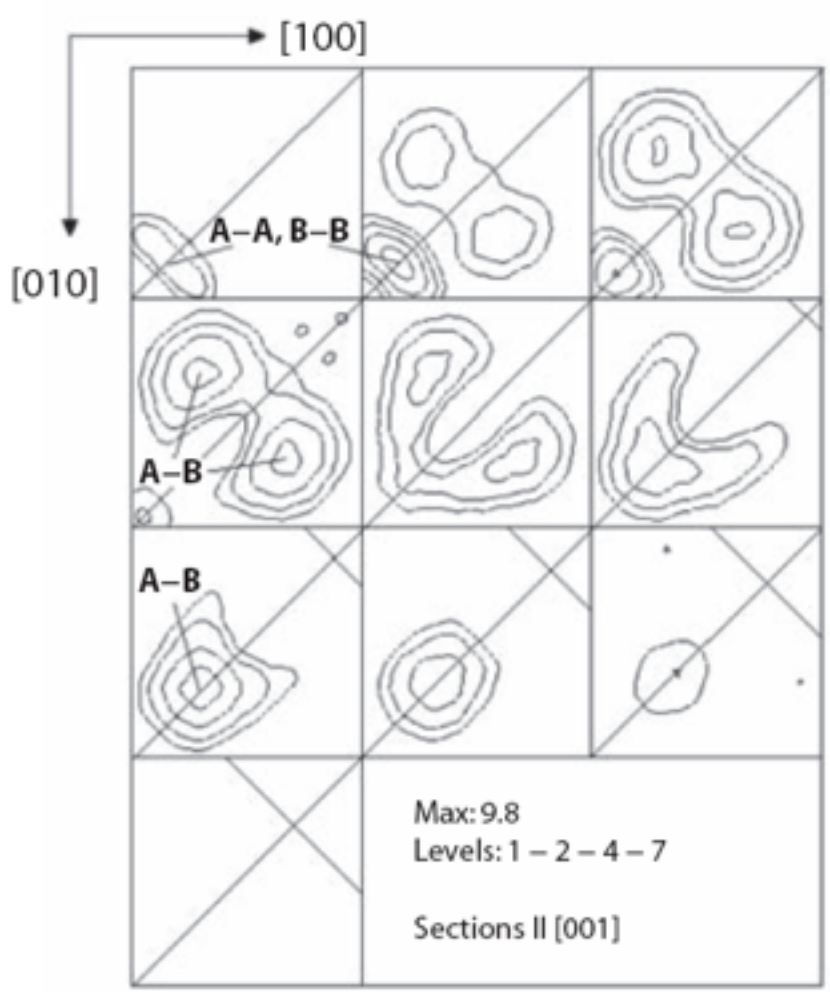

(c)

MODF

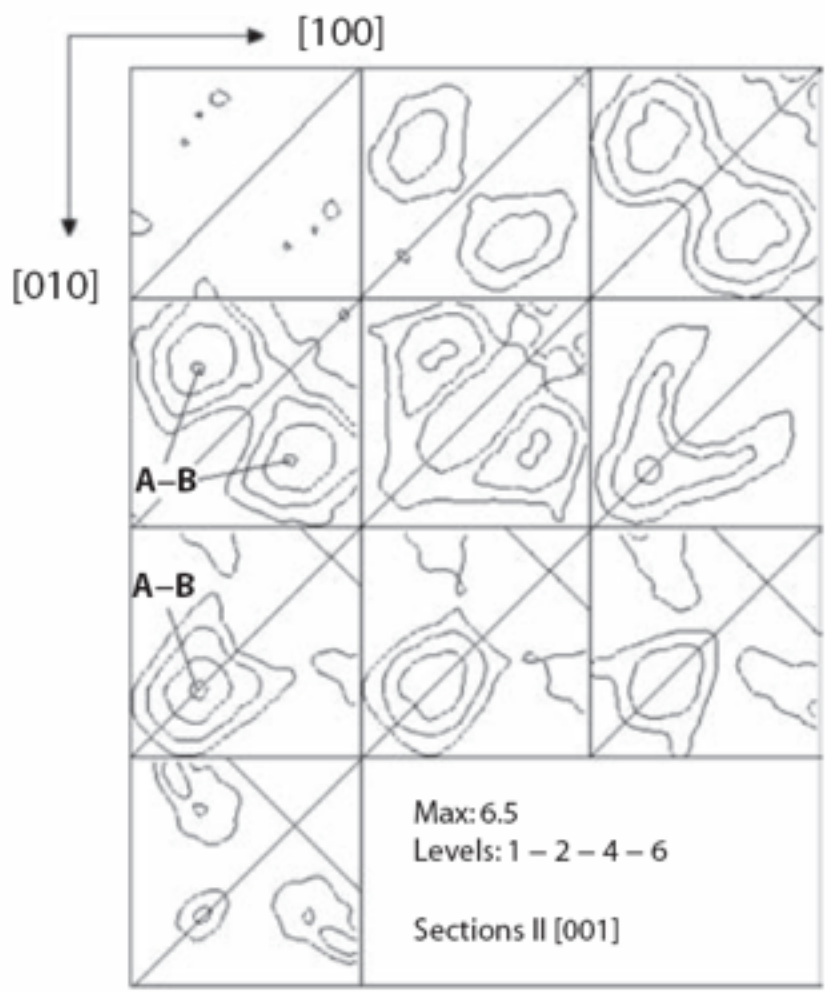

(d)

OCF

MODF, ODDF and Mackenzie distribution

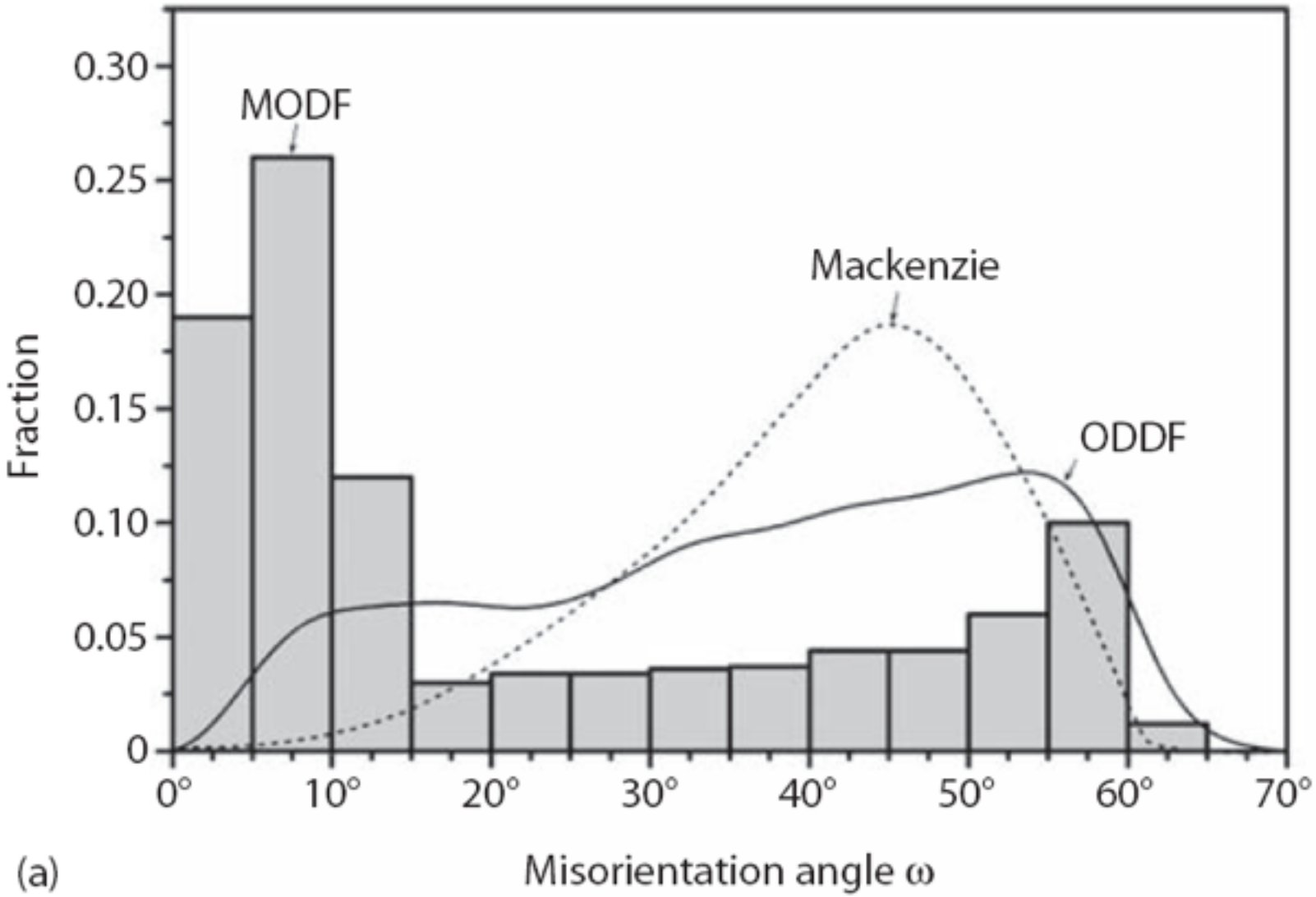

MODF and OCF

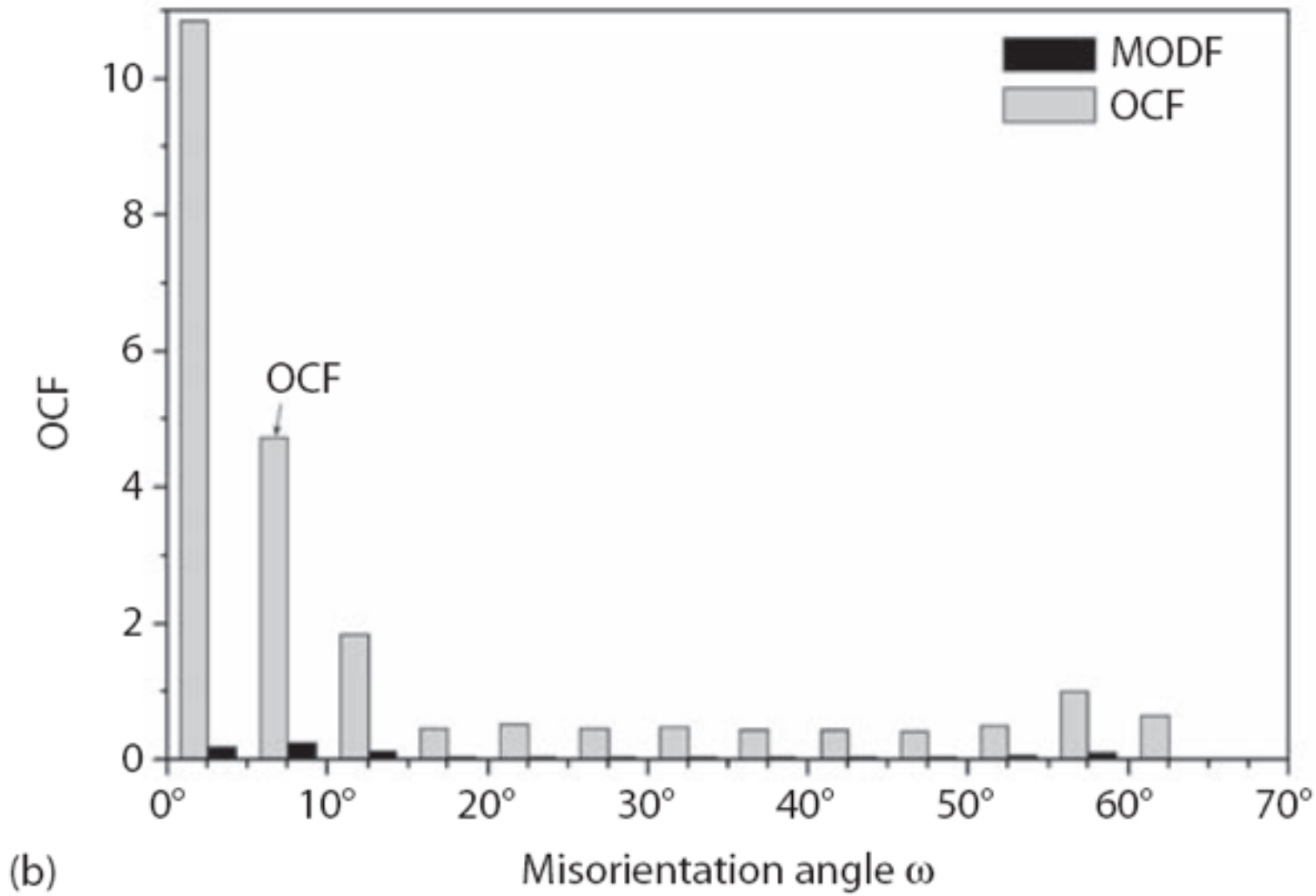
MODF
OCF
OCF
OCF
10
8
6
4
2
0
0°
10°
20°
30°
40°
50°
60°
70°
(b)
Misorientation angle ω

Extracted texture components

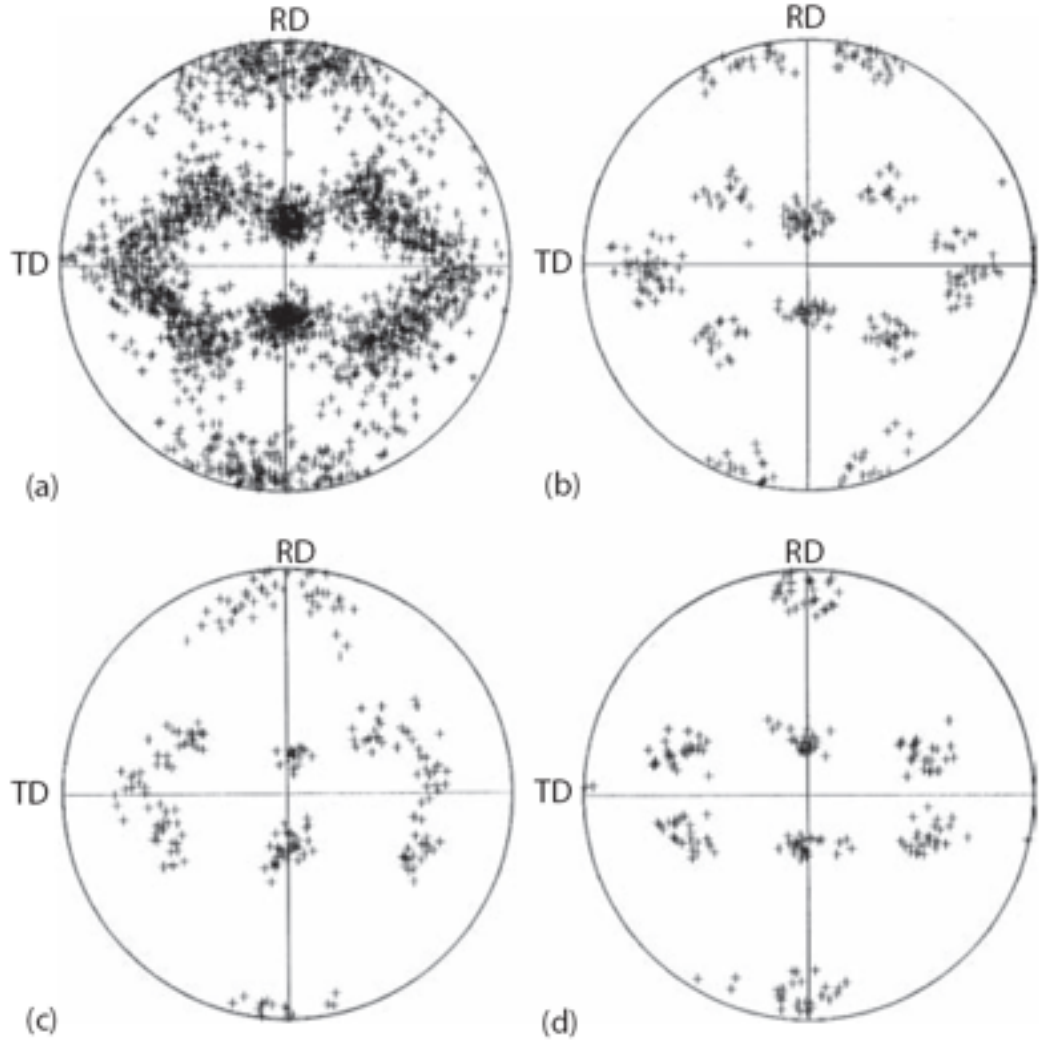

(a) {111} Pole figure from deformed and part annealed aluminum. Some of the texture components are extracted onto separate pole figures, using a 15° spread. (b) {123}⟨634⟩, (c) {211}⟨111⟩, (d) {436}⟨323⟩. See also Table 9.3. (Data from Davies, R. and Randle, V., *Mater. Char.*, 37, 131, 1996.)

Texture components

Proportion (%) of Grains Representative of Each Main Texture Component from the Data in Figure 9.23a

Orientation	{001} ⟨100⟩	{001} ⟨310⟩	{103} ⟨311⟩	{101} ⟨111⟩	{211} ⟨111⟩	{123} ⟨634⟩	{436} ⟨323⟩	Random
Proportion [%]	8.7	3.3	4.3	4.7	21.0	28.0	19.3	10.7

Source: Data from Davies, R. and Randle, V., *Mater. Char.*, 37, 131, 1996.